bjh research paper

Pro-inflammatory cytokines favor the emergence of ETV6-RUNX1-positive pre-leukemic cells in a model of mesenchymal niche

Linda Beneforti,[1] Erica Dander,[1] Silvia Bresolin,[2] Clara Bueno,[3] Denise Acunzo,[1] Mayla Bertagna,[1] Anthony Ford,[4] Bernhard Gentner,[5] Geertruy te Kronnie,[2] Patrizia Vergani,[6] Pablo Menéndez,[3,7,8] Andrea Biondi,[1,9] Giovanna D'Amico,[1] Chiara Palmi[1,*] and Giovanni Cazzaniga[1,*]

[1]Centro Ricerca Tettamanti, University of Milano-Bicocca, MBBM Foundation, [2]Dipartimento della Salute della Donna e del Bambino, University of Padua, Padua, [3]Department of Biomedicine, School of Medicine, Josep Carreras Leukemia Research Institute, University of Barcelona, [4]Centre for Evolution and Cancer, The Institute of Cancer Research, London, UK, [5]San Raffaele Telethon Institute for Gene Therapy (SR-TIGET), IRCCS San Raffaele Scientific Institute, Milan, [6]Dipartimento di Ostetricia, MBBM Foundation, [7]Institució Catalana de Recerca i Estudis Avançats (ICREA), [8]Centro de Investigación Biomédica en Red de Cáncer (CIBER-ONC), ISCIII, Barcelona, Spain and [9]Clinica Pediatrica, MBBM Foundation, University of Milano-Bicocca, Monza, Italy

Received 19 September 2019; revised 19 December 2019; accepted for publication 13 January 2020

Correspondence: Dr Giovanni Cazzaniga and Dr Chiara Palmi, Centro Ricerca M. Tettamanti, Pediatric Clinic, University of Milano Bicocca, MBBM Foundation, Via Pergolesi 33, 20900 Monza (MB), Italy.
E-mail: c.palmi@asst-monza.it; gianni.cazzaniga@asst-monza.it

*C.P. and G.C. contributed equally to this work

Summary

ETV6-RUNX1 (E/R) fusion gene, arising *in utero* from translocation t(12;21)(p13:q22), is the most frequent alteration in childhood acute lymphoblastic leukemia (ALL). However, E/R is insufficient to cause overt leukemia since it generates a clinically silent pre-leukemic clone which persists in the bone marrow but fails to out-compete normal progenitors. Conversely, pre-leukemic cells show increased susceptibility to transformation following additional genetic insults. Infections/inflammation are the most accredited triggers for mutations accumulation and leukemic transformation in E/R^+ pre-leukemic cells. However, precisely how E/R and inflammation interact in promoting leukemia is still poorly understood. Here we demonstrate that IL6/TNFα/ILβ pro-inflammatory cytokines cooperate with BM-MSC in promoting the emergence of E/R^+ Ba/F3 over their normal counterparts by differentially affecting their proliferation and survival. Moreover, IL6/TNFα/ILβ-stimulated BM-MSC strongly attract E/R^+ Ba/F3 in a CXCR2-dependent manner. Interestingly, E/R-expressing human $CD34^+IL7R^+$ progenitors, a putative population for leukemia initiation during development, were preserved in the presence of BM-MSC and IL6/TNFα/ILβ compared to their normal counterparts. Finally, the extent of DNA damage increases within the inflamed niche in both control and E/R-expressing Ba/F3, potentially leading to transformation in the apoptosis-resistant pre-leukemic clone. Overall, our data provide new mechanistic insights into childhood ALL pathogenesis.

Keywords: ALL, ETV6-RUNX1, pre-leukemia, MSC, inflammation.

First published online 2 March 2020
doi: 10.1111/bjh.16523

Introduction

ETV6-RUNX1 (E/R), generated from translocation t(12;21) (p13;q22) (Golub *et al*, 1995; Romana *et al*, 1995), is the most frequent fusion gene in pediatric cancer (Inaba *et al.*, 2013), exclusively leading to B-cell precursors acute lymphoblastic leukemia (BCP-ALL) (Mullighan, 2013). Translocation occurs *in utero* in 2–5% of healthy newborns (Ford *et al.*, 1998; Wiemels *et al.*, 1999; Schäfer *et al.*, 2018) and drives the expansion of a pre-leukemic clone that contributes to hematopoiesis but fails to out-compete the normal counterpart (Tsuzuki *et al*, 2004; Hong *et al*, 2008; Schindler *et al*, 2009). On the other hand, pre-leukemic cells show increased susceptibility to additional genetic insults, leading to leukemia in about 1% of E/R carriers (Inaba *et al.*, 2013; Kantner *et al.*, 2013). Importantly, secondary mutations in the original, chemoresistant pre-leukemic clone are supposed to be responsible for E/R$^+$ long-term relapses (Levasseur et al., 1994; Ford *et al.*, 2001; Konrad *et al.*, 2003; Kuster *et al.*, 2018).

Epidemiological and experimental data indicate that infections/inflammation are the most accredited triggers for malignant progression in E/R$^+$ pre-leukemic cells (Heath &Hasterlik, 1963; Francis *et al.*, 2012; Cazzaniga *et al.*, 2017). Regarding this, we previously showed that TGFβ, a pleiotropic cytokine produced under inflammation (Yoshimura *et al.*, 2010), favored the emergence of E/R-expressing cells against controls in competitive growth assays (Ford *et al.*, 2009). More recently, it has been demonstrated that E/R pre-leukemic mice developed BCP-ALL when exposed to common facilities (Rodríguez-Hernández *et al*, 2017; Ford, unpublished observations), while E/R$^+$ pre-B cells subjected to repetitive LPS-stimulation induced leukemia when transplanted in mice (Swaminathan *et al*, 2015).

It is well known that both normal and malignant hematopoietic stem-progenitor cells (HSPC) are strictly regulated by BM-derived signals (Méndez-Ferrer *et al.*, 2010; Lilly *et al.*, 2011; Asada, 2018). Of note, we have previously suggested that may affect pre-leukemic cells interactions with the BM stroma by altering their adhesive and migratory properties (Palmi *et al*, 2014). In addition to function as important modulators of inflammation (Bernardo & Fibbe, 2013), BM-mesenchymal stromal cells (MSC) have gained great interest for their active role in leukemia pathogenesis (Lo *et al.*, 2014; Polak *et al.*, 2015; Naderi *et al.*, 2015; De Rooij *et al.*, 2017). In particular, it has been shown that BM-MSC alterations are able to induce genotoxic stress in HSPC leading to hematological malignancies (Raaijmakers *et al*, 2010; Zambetti *et al*, 2016).

Here we took advantage of two E/R-expressing cellular systems to demonstrate that BM-MSC and IL6/IL1β/TNFα pro-inflammatory cytokines cooperate in favoring the emergence of E/R$^+$ pre-leukemic cells in addition to predisposing them to malignant transformation.

Methods

E/R-inducible Ba/F3 model

E/R-expressing and control Ba/F3 clones were a kind gift of Dr A.M. Ford. Briefly, the mifepristone-inducible GeneSwitch system (Life Technologies, Carlsbad, USA) was used to express E/R fused to the V5 epitope. E/R expression efficiency (>80%) were verified by flow-cytometry using a FITC-conjugated anti-V5 antibody (Abcam, Cambridge, UK) (Ford *et al.*, 2009).

Competitive mesenchymal niche model

Control and E/R$^+$ Ba/F3 were mixed (2.5×10^4 total cells) at a starting ratio of 20:80%, plated in different culture conditions for 96 h and analyzed by flow-cytometry (details in Data S1).

Migration assay

Control and E/R$^+$ Ba/F3 (3×10^5) were resuspended in 100 μl of migration medium (Advanced RPMI, 2% FBS, 1% L-glutamine) and loaded into the upper chamber of 8·0 μm Transwells® inserts (Corning, MA, USA). Unstimulated or inflamed BM-MSC supernatants (600 μl) were added to the lower chamber. Details are in Data S1.

Cell cycle analysis

Control and E/R$^+$ Ba/F3 (0.5×10^6) were stained with 2·5 μM carboxyfluorescein succinimidyl ester (CFSE). 2.5×10^4 stained cells were mixed (20%ctr:80%E/R$^+$) and cultured under basal condition or on murine BM-MSC in the presence or absence of IL6/IL1β/TNFα. After 4 days, CFSE mean fluorescence intensity (MFI) was determined. Details are in Data S1.

Apoptosis and DNA damaging assays

Mixed control and E/R$^+$ Ba/F3 cells (20%:80%, 2.5×10^4 tot) were cultured under basal condition or on BM-MSC in the presence or absence of IL6/IL1β/TNFα. After 4 days, the percentage of annexin V-negative cells was determined by flow-cytometry. Details are in the Supplementary Materials.

Transduced UCB-CD34$^+$ and BM-MSC co-cultures

Sorted pRRL-GFP and pRRL-E/R-GFP-transduced UCB-CD34$^+$ cells (see Supplementary Materials for details) were resuspended in stem culture medium (StemSpam SFEM-II, StemCell Technologies, Vancouver, Canada, supplemented with SCF, FLT3-ligand, IL3, IL6 and TPO) and plated on human BM-MSC in presence or absence of IL6/IL1β/TNFα for 72 h. Details are in the Supplementary Materials.

Statistical Analysis

Student's *t*-test with $P < 0{\cdot}05$ was used to define statistically significant results. To compare variances between groups, the F test was performed; in case of significantly different variances, the Welch's correction was applied. Where indicated, one-sample *t*-test was used with the same significance threshold.

Results

IL6/IL1β/TNFα-mediated inflammation favors the emergence of the E/R$^+$ pre-leukemic clone in an in vitro *model of competitive mesenchymal niche*

In order to investigate if BM-MSC and inflammation cooperate in favoring the emergence of E/R$^+$ pre-leukemic cells, we performed competitive growth assays as we previously did to evaluate the effect of TGFβ (Ford *et al.*, 2009). E/R-expressing (E/R$^+$) and control (ctr) Ba/F3 cells were mixed at a starting ratio of 80%:20%, in consideration of the proliferative disadvantage of the first (Ford *et al.*, 2009). The mix was then plated on murine BM-MSC (a system hereafter indicated as "competitive mesenchymal niche"), with or without IL6/IL1β/TNFα pro-inflammatory cytokines as a general inflammatory stimulus (Swiergiel & Dunn, 1999; Cappuzzello *et al.*, 2016; Scutera *et al.*, 2018; Portale *et al.*, 2019) (Fig S1). Standard liquid cultures without factors (basal condition) or with TGFβ were performed as experimental controls. In agreement with our previous findings, the percentage of E/R$^+$ Ba/F3 decreased after 96 h in basal condition compared to day 0 (28%±14% E/R$^+$). To the contrary, however, E/R$^+$ cells achieved a numerical parity with control cells in the presence of TGFβ (50%±20% E/R$^+$, $P < 0{\cdot}01$) (Ford *et al.*, 2009). Co-culturing the mix on unstimulated BM-MSC provided the same result of basal condition (21%±12 % E/R$^+$, $P = ns$), while, interestingly, the addition of IL6/IL1β/TNFα within the competitive mesenchymal niche significantly increased the percentage of E/R$^+$ Ba/F3 (47%±17% E/R$^+$, $P < 0{\cdot}01$). Of note, the effect of IL6/IL1β/TNFα was dose-dependent and relied on the presence of the mesenchymal component, since no advantage on E/R$^+$ Ba/F3 was observed by exposing the mix to IL6/IL1β/TNFα *in the absence* of BM-MSC (27%±12% E/R$^+$, $P = ns$) (Figs 1 and S2). Moreover, we stimulated the competitive mesenchymal niche with the single cytokines or with the double combinations. As shown in Fig S2, the addition of single cytokines or IL1β/IL6 did not induce modifications in the mix compared to the unstimulated niche, while stimulation with TNFα/IL6 and, particularly, TNFα/IL1β provided a significant advantage on E/R-expressing cells, albeit to a lesser extent compared to IL6/IL1β/TNFα. Since it has been demonstrated that lipopolysaccharide (LPS) promotes E/R-driven leukemogenesis *in vivo* (Swaminathan *et al*, 2015), we also wanted to test this infective agent in our competitive mesenchymal niche model, in addition to other well-known infective/inflammatory stimuli such as IFNα, Poly (I:C), PAM3CSK4 and S100A8/9. Except for a slight increase in the case of Poly (I:C), we did not observe differences compared to unstimulated BM-MSC (Figs S2 and S3). To countercheck the role of pro-inflammatory cytokines in our observations, we treated the mesenchymal competitive niche with the anti-inflammatory cytokine IL10. As shown in Fig S2, however, addition of IL10 did not alter the mix composition compared to the unstimulated niche.

Finally, we investigated if soluble factors rather than cell-cell contacts mediated the pre-leukemia-advantaging effect within the IL6/IL1β/TNFα-stimulated competitive mesenchymal niche. As shown in Fig S4A, no differences emerged by performing experiments on 0·4 μm Transwell® compared to direct co-cultures, indicating that secreted factors played the major role. Notably, an involvement of TGFβ could be ruled out, since its concentration in BM-MSC supernatants did not increase after IL6/IL1β/TNFα stimulation (Fig S4B).

The inflamed mesenchymal niche preferentially attracts E/R$^+$ B-progenitors through the CXCR2 receptor

Our preliminary studies on human BM-MSC showed that IL6/TNFα/IL1β stimulation induced a strong release of CXCL1 and other CXCR1/2-binding chemokines (Fig 2A, grey rows; Table S1). Accordingly, murine BM-MSC increased secretion of CXCL1 after IL6/TNFα/IL1β stimulation (inflamed: 28199 ± 3098 pg/ml; unstimulated: 60 ± 16 pg/ml; $P < 0{\cdot}01$) (Fig 2B). On the other hand, gene expression profile of E/R$^+$ and control Ba/F3 (Fig S5A) revealed that pre-leukemic cells activated pathways involved in inflammatory responses and myeloid-cells activation, including the CXCR2 signaling (Figs S5B–S5C). Indeed, E/R$^+$ Ba/F3 transcriptionally upregulated *CXCR2* and its cognate receptor *CXCR1* (Rosu-Myles *et al*, 2000; Stillie *et al*, 2009) (*CXCR1* mRNA fold increase E/R$^+$ *versus* ctr = 55·3 ± 7·9, $P < 0{\cdot}001$; *CXCR2* mRNA fold increase E/R$^+$ *versus* ctr = 140·2 ± 45·2, $P < 0{\cdot}001$), but they expressed only the first at the membrane surface (CXCR2 MFI: E/R$^+$= 1378 ± 807; ctr = 284±167, $P < 0{\cdot}05$) (Fig 3A–B). Interestingly, E/R-positive patients expressed higher levels of *CXCR2* mRNA than E/R-negative ones (Fig S6).

CXCR2 regulates survival and self-renewal of normal HSPC as well as AML stem cells (Schinke *et al*, 2015; Sinclair *et al*, 2016). However, blocking CXCR2 with the specific inhibitor SB265610 did not abolish the advantage of E/R$^+$ Ba/F3 in the presence of BM-MSC and IL6/IL1β/TNFα (Fig S7). Likewise, addition of CXCL1 in standard liquid culture did not increase the percentage of pre-leukemic cells (Fig S8).

CXCR2 primarily mediates neutrophil migration to sites of inflammation (Richardson *et al*, 2003); in addition, it represents a selective migratory pathway for BCP-ALL blasts toward the leukemic niche (De Rooij *et al*, 2017). Since we previously showed that E/R altered cell migration (Palmi *et al*, 2014), we asked if CXCR2 overexpression was associated with increased migration of E/R$^+$ Ba/F3 towards inflamed BM-MSC. As shown

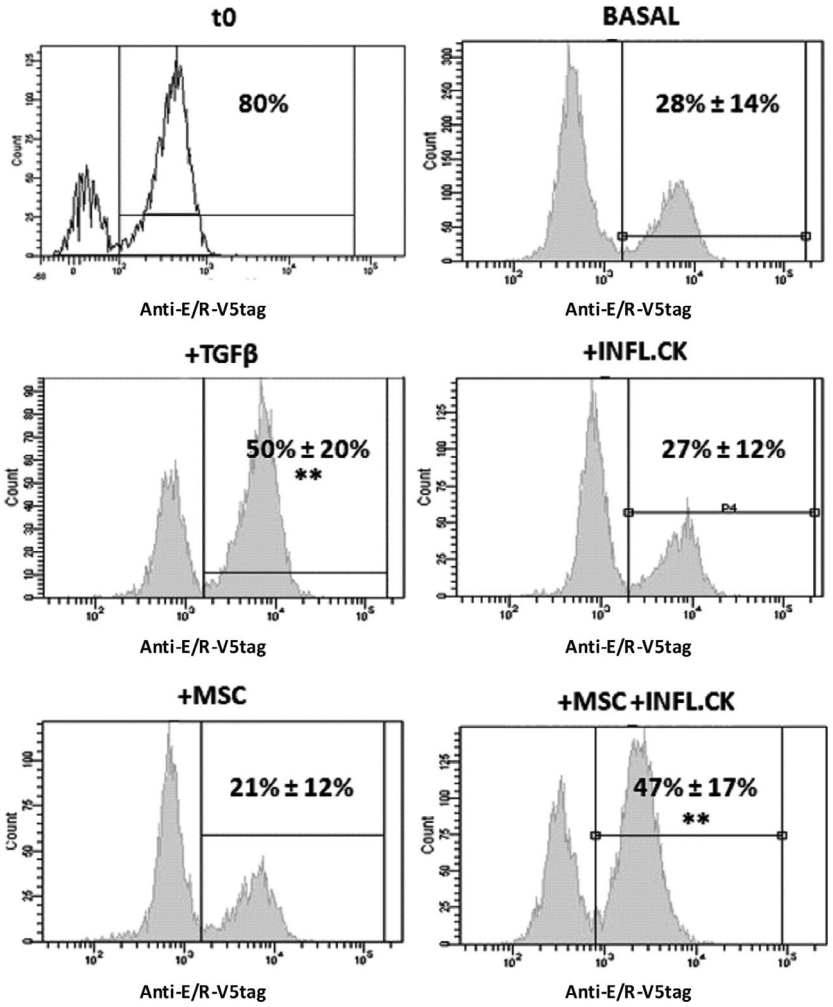

Fig 1. Pro-inflammatory cytokines favor the emergence of E/R$^+$ Ba/F3 cells in a model of competitive mesenchymal niche. A mixture of E/R$^+$ and control Ba/F3 cells (80%:20%) was grown under the indicated conditions. BASAL: standard liquid culture; +TGFβ: standard liquid culture + TGFβ (10 ng/mL); + inflammatory cytokines (INFL. CK): standard liquid culture + IL6 (20 ng/mL), TNFα (25ng/mL) and IL1β (25 ng/mL); +MSC: Ba/F3 and murine BM-MSC co-culture; +MSC + INFL.CK: Ba/F3 and murine BM-MSC co-culture + IL6, TNFα and IL1β. After 4 days, the percentage of E/R$^+$ cells in the mix was quantified by flow-cytometry using a FITC-conjugated anti-V5 tag antibody. An anti-mCD45 was used to discriminate between MSC (mCD45$^-$) and Ba/F3 cells (mCD45$^+$). Peak histograms in the figure are from a representative experiment, while values indicate mean ± SD of 6 independent experiments. Paired Student's *t*-test (two-sided, $^{**}P < 0{\cdot}01$) was applied to compare the percentage of E/R$^+$ cells grown for 4 days under the indicated conditions *vs* the basal culture.

in Fig 4, both normal and pre-leukemic Ba/F3 cells migrated more towards inflamed BM-MSC supernatants compared to unstimulated BM-MSC conditioned media, despite the increase being significant only in the latter case (% control migrated cell/input: MSC-CM = 5·9 ± 2·9; INFL.MSC-CM: 14·3 ± 9·6, $P = ns$) (% E/R$^+$ migrated cell/input: MSC-CM = 4·6 ± 3·3; INFL.MSC-CM: 30·2 ± 9, $P < 0{\cdot}01$). In particular, E/R$^+$ cells migrated 2-fold more efficiently towards inflamed MSC-CM compared to controls (% migrated cell/input toward INFL.MSC-CM: E/R$^+$=30·2 ± 9·1; ctr = 14·3 ± 9·6, $P < 0{\cdot}01$). On the other hand, no significant differences were observed between control and E/R$^+$ Ba/F3 in case of unstimulated MSC-CM (% migrated cell/input toward MSC-CM: E/R$^+$=4·6 ± 3·3; ctr = 5·9 ± 2·9, $P = ns$). As expected, CXCR2 inhibition hampered migration of E/R$^+$ Ba/F3: of note, the inhibitory effect was not statistically significant in case of unstimulated MSC supernatants (%E/R$^+$ migrated cells/input: -SB265610 = 4·6 ± 3·3; +SB265610 = 2·2 ± 1·3, $p = ns$), whereas it was significantly consistent in the presence of inflamed supernatants (% E/R$^+$ migrated cells/input: -SB265610 = 30·2 ± 9; +SB265610 = 7·7 ± 4·3; $P < 0{\cdot}01$). In stark contrast, migration of control Ba/F3 was not significantly affected by CXCR2 inhibition in both conditions.

Proliferation and survival of normal, but not E/R$^+$, pro-B cells strongly decrease in the presence of BM-MSC and IL6/TNFα/IL1β

In order to elucidate mechanisms underlying the emergence of pre-leukemic Ba/F3 within the competitive inflamed niche, we

(A)

	FC	*p-value*
CXCL1 (GROalpha)	**304·99**	***0·018***
GRO-family	**14·30**	***0·003***
CXCL8	**12·02**	***0·001***
GM-CSF	10·33	*0·061*
betaFGF	9·32	*0·011*
CXCL6	**8·77**	***0·045***
CCL5	6·29	*0·064*
betaNGF	5·65	*0·051*
CXCL5	**4·77**	***0·007***
HGF	4·00	*0·025*

(B)

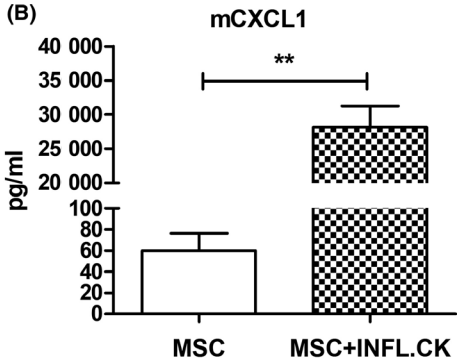

Fig 2. BM-MSC increase secretion of CXCR1/2 ligands after stimulation with pro-inflammatory cytokines. A) Human BM-MSCs from three different healthy-donors were grown in 2% FBS-supplemented media in presence or absence of IL6 (40 ng/mL), IL1β (50 ng/mL) and TNFα (100 ng/mL) for 24 h. Conditioned media (CM) were collected, centrifuged, and analyzed by Human Cytokines Array C1000 protein arrays (RayBio). Data were acquired through the UVITEC Cambridge® instrument and densitometry quantification performed by ImageJ® software. For each donor, protein fold-changes (FC) of inflamed *vs* unstimulated supernatants were calculated. The table shows the FC mean values of the 10 most upregulated proteins obtained in three independent experiments. CXCR1/2 ligands are indicated in grey. B) CXCL1 quantification by enzyme-linked immunosorbent assay (ELISA) in the supernatants of murine BM-MSCs grown in 2% FBS-supplemented media in the absence (MSC) or presence of IL6, TNFα and IL1β (MSC + INFL.CK) for 24 h. Values are shown as mean ± SD of 3 independent experiments. Paired Student's t-test: two-sided, $^{**}P < 0{\cdot}01$.

analyzed proliferation and apoptosis in control and E/R$^+$ Ba/F3 when exposed to that microenvironment (Fig 5A). Consistent with our previous report (Ford *et al.*, 2009), E/R$^+$ Ba/F3 cultured in basal condition for 96 h displayed a lower proliferative rate than control cells, as judged by higher CFSE intensity. Of note, comparable results were observed by co-culturing the mix (20% ctr:80% E/R$^+$) on unstimulated BM-MSC. Interestingly, both populations decreased proliferation compared to the unstimulated condition if cultivated on BM-MSC + IL6/IL1β/TNFα. However, decrease was stronger in control (CFSE MFI fold change + MSC+INFL.CK *vs* + MSC: ctr = 4·4 ± 1·8, $P < 0{\cdot}05$) than pre-leukemic Ba/F3 (CFSE MFI fold change + MSC+INFL.CK *vs* + MSC: E/R$^+$=2·2 ± 0·6, $P < 0{\cdot}001$). Very interestingly, a striking difference was observed in terms of apoptosis: cell death, in fact, was strongly induced in control cells exposed to the inflamed niche (% ANN-V-negative cells: +MSC = 68·4 ± 5·7; +MSC + INFL.CK = 48·2 ± 1·3, $P < 0{\cdot}05$), whereas survival of E/R$^+$ cells was completely unaffected in the same condition (Fig 5B).

Human normal, but not E/R$^+$, CD34$^+$IL7R$^+$ progenitors decrease in number in the presence of BM-MSC and IL6/TNFα/IL1β

Although inducible E/R-expressing Ba/F3 cells proved to be a reliable system to study E/R$^+$ pre-leukemia (Diakos *et al.*, 2007; Ford *et al.*, 2009; Linka *et al.*, 2013; Palmi *et al.*, 2014), we wanted to test the effects of BM-MSC and IL6/IL1β/TNFα also in a human pre-leukemic cellular model. It has recently been demonstrated that fetal CD34$^+$CD19$^-$IL7R$^+$ progenitors are the *bona fide* initiating population of E/R$^+$ pre-leukemia during development (Böiers *et al*, 2018). We thus transduced umbilical cord blood-CD34$^+$ progenitors with pRRL-GFP or pRRL-E/R-GFP lentiviral vectors (control or E/R$^+$ UCB-CD34$^+$ respectively) and separately cultured them for 72 h on human BM-MSC in the presence or absence of IL6/IL1β/TNFα. By adopting this short-term culture system, the whole population lacked CD19 expression; on the contrary, a CD34$^+$IL7R$^+$ subpopulation clearly emerged in both control and pre-leukemic cells (Fig S9A, gate P7). In line with previous findings (Böiers *et al*, 2018), expression of the E/R itself led to a specific expansion of the CD34$^+$IL7R$^+$ compartment (Fig 6B, upper graph; control CD34$^+$IL7R$^+$=373 ± 101; E/R$^+$ CD34$^+$IL7R$^+$= 635 ± 44, $P < 0{\cdot}05$), while it had no significant impact on the CD34$^+$IL7R$^-$ and CD34$^-$ fractions.

Addition of IL6/IL1β/TNFα to control UCB-CD34$^+$/BM-MSC co-cultures increased the number of total GFP$^+$ cells (tot control GFP$^+$: +MSC = 6117±1646; +MSC + INFL.CK = 8077±1087; $P < 0{\cdot}05$). Such increase was accompanied by the expansion of differentiating CD34$^-$ cells and a significant reduction of control CD34$^+$IL7R$^+$ progenitors (control CD34$^-$: +MSC = 3649±963; +MSC + INFL.CK: 5516 ± 622, $P < 0{\cdot}05$; control CD34$^+$IL7R$^+$ number: +MSC = 373±101; +MSC + INFL.CK: 254 ± 56, $P < 0{\cdot}05$; control CD34$^+$IL7R$^+$ percentage: +MSC = 6·1% ±0·5%; +MSC + INFL.CK: 3·1%±0·3%, $P < 0{\cdot}01$). Notably, any alterations were observed in the control CD34$^+$IL7R$^-$ subpopulation (Fig 6A, lower graph).

Very interestingly, in the presence of BM-MSC and IL6/TNFα/IL1β, E/R-expressing CD34$^+$IL7R$^+$ progenitors were preserved from reduction (E/R$^+$ CD34$^+$IL7R$^+$: +MSC = 635±44; +MSC + INFL.CK: 727 ± 142, $P = ns$) (Fig 6B, lower graph). On the other hand, the number of total pre-leukemic GFP$^+$ cells decreased (tot E/R$^+$ GFP$^+$: +MSC + INFL.CK = 6374 ± 997; +MSC = 6727±1300; $P < 0{\cdot}05$), possibly due to a reduction of the CD34$^-$ fraction (E/R$^+$ CD34$^-$: +MSC = 4403 ± 726; +MSC + INFL.CK: 3615 ± 542, $P < 0{\cdot}05$). As in the control group, E/R$^+$ CD34$^+$IL7R$^-$ cells were unaffected compared to the uninflamed niche.

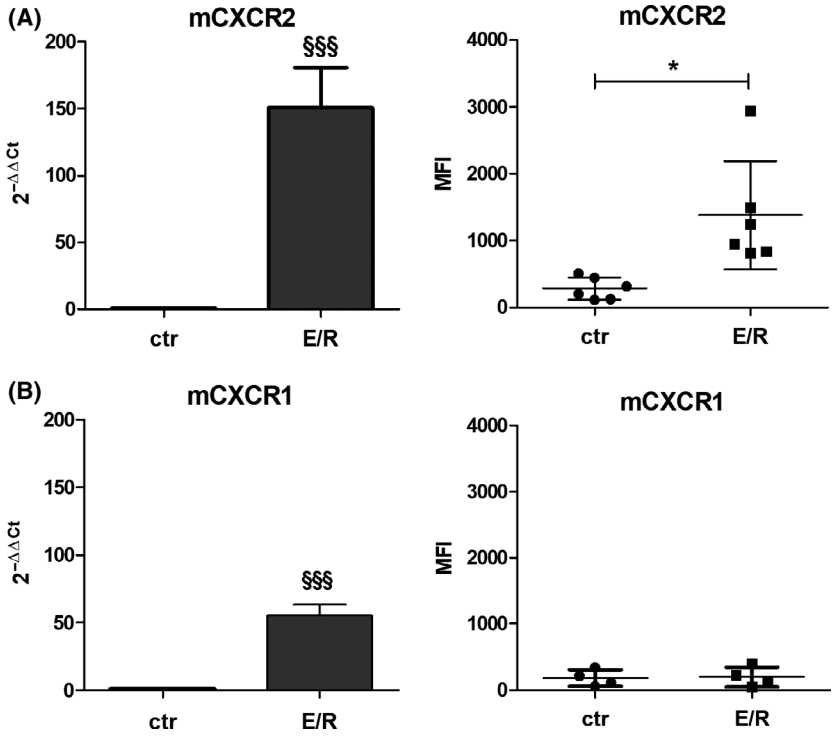

Fig 3. Overexpression of *CXCR2* mRNA and cell surface protein in E/R$^+$ Ba/F3 cells. A) RT-qPCR analysis of *CXCR1* and *CXCR2* mRNA expression in control and E/R$^+$ Ba/F3 cells after 72 h of mifepristone treatment. cDNA was subjected to TaqMan qRT-PCR and normalized for *HPRT* gene expression. Values are shown as mean ± SD of 6 independent experiments; for each experiment, the $2^{-\Delta\Delta Ct}$ value of Ba/F3 control was considered as reference. One-sample *t*-test: $^{§§§}P < 0{\cdot}001$. B) CXCR1 and CXCR2 protein membrane expression was quantified as mean fluorescence intensity (MFI) by FACS analysis. In the scattered dot plot, values are expressed as mean ± SD of 6 independent experiments. Student's *t*-test with Welch's correction: two-sided, $^{*}P < 0{\cdot}05$.

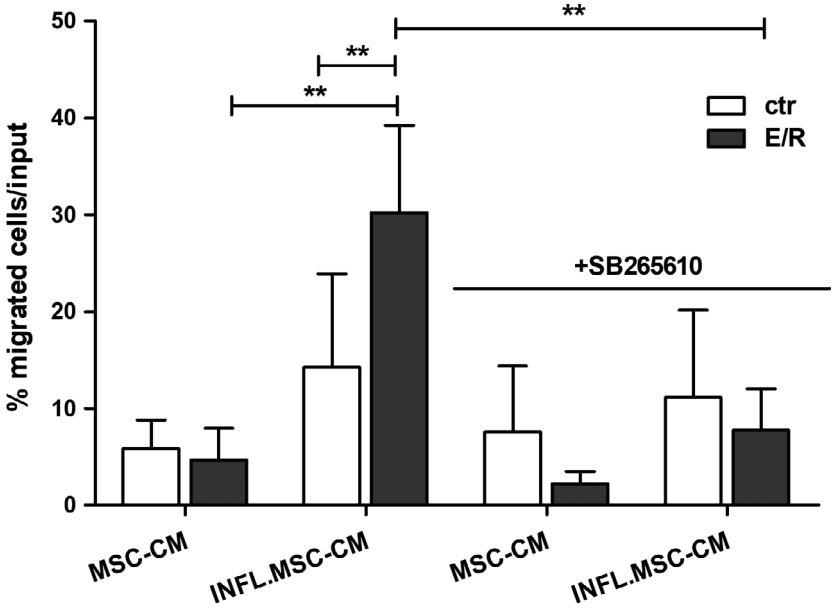

Fig 4. Enhanced migration of E/R$^+$ Ba/F3 cells towards inflamed BM-MSC conditioned medium is CXCR2-dependent. Transwell® migration (3 h) of control and E/R$^+$ Ba/F3 towards basal (MSC-CM) or inflamed (INFL.MSC-CM) MSC supernatant in the presence or absence of the CXCR2-inhibitor SB265610 (1 μM). The number of migrated cells was determined by flow cytometry. A set number of fluorescent reference beads (BD Trucount® tubes) was used as internal calibrator, as described in the Material and Methods. Cells were counted in technical triplicates for 30 s. The percentage of migrated cells was determined by dividing the number of cells in the lower chamber by the number of cells loaded into the upper chamber (input). Values are given as mean ± SD of 5 independent experiments. Paired Student's *t*-test: two-sided, $^{**}P < 0{\cdot}01$.

Since a CD34^{high}IL7R$^+$ phenotype was recognisable in control and E/R$^+$ UCB-CD34$^+$-derived populations (Fig S9A, gate P8), we extended the analysis to these fractions as well. Similar to the CD34$^+$IL7R$^+$ compartment, in the presence of BM-MSC + IL6/TNFα/IL1β, CD34^{high}IL7R$^+$ progenitors significantly decreased in controls (fold-change control + MSC+ INFL.CK *vs* + MSC=0·63 ± 0·07; $P < 0{\cdot}05$) while they were unaffected in number within the pre-leukemic population (fold-change E/R$^+$ +MSC + INFL.CK *vs* + MSC=1·09 ± 0·03; $P < 0{\cdot}05$, Fig S9B).

The inflamed mesenchymal niche represents a genotoxic microenvironment for hematopoietic progenitors

It has been demonstrated that mesenchymal inflammation induces genotoxic stress in HSPC (Zambetti *et al*, 2016).

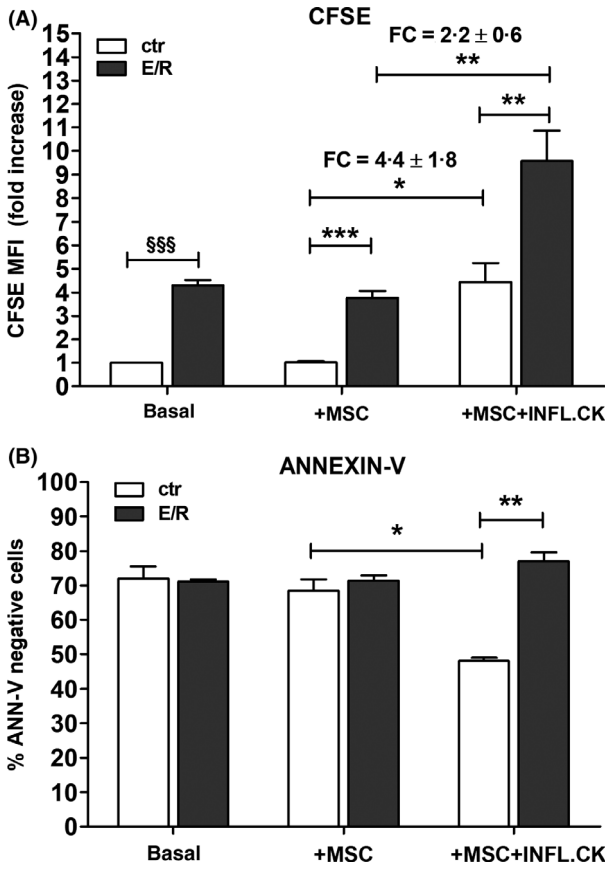

Fig 5. Differential effect of the inflamed mesenchymal niche on the proliferation and survival of control and E/R$^+$ Ba/F3 cells. A) E/R$^+$ and control Ba/F3 cells were stained with carboxyfluorescein succinimidyl ester (CFSE) and co-cultured (80%:20%) for 4 days in standard liquid culture (basal) or on murine BM-MSC monolayers in the presence or absence of IL6/TNFα/IL1β. CFSE MFI of mCD45$^+$ cells was evaluated by flow cytometry. The E/R$^+$ fraction was detected thanks to a specific antibody against the E/R fusion sequence in place of the FITC-conjugated anti-V5 antibody. MFI of control Ba/F3 in basal condition at the end of the culture was considered as reference for fold increase calculation. The graph shows mean ± SD of 5 independent experiments. $^{§§§}P < 0{\cdot}001$, one-sample t-test; paired Student's *t*-test: $^{*}P < 0{\cdot}05$; $^{**}P < 0{\cdot}01$; $^{***}P < 0{\cdot}001$. FC: fold change B) E/R$^+$ and control Ba/F3 (80%:20%) were grown as above in the presence or absence of inflammatory cytokines. For each condition, the percentage of mCD45$^+$/annexin V$^-$ cells was evaluated, and E/R + cells quantified using the FITC-conjugated anti-V5 antibody. The graph shows mean ± SD of 3 independent experiments: Paired Student's *t*-test: two-sided, $^{*}P < 0{\cdot}05$; $^{**}P < 0{\cdot}01$.

Thus, we sought to determine the extent of DNA Double-Strand Break (DSB) in control and E/R$^+$ Ba/F3 in the presence of BM-MSC and IL6/TNFα/IL1β. As judged by the levels of histone 2AX phosphorylation (γH2AX), under basal conditions, pre-leukemic cells were characterized by higher levels of DNA DSB compared to controls (γH2AX MFI fold increase: E/R$^+$ *vs* ctr = 1·86 ± 0·65, $P < 0{\cdot}05$) (Fig 7A). Interestingly, exposure to unstimulated BM-MSC did not affect basal γH2AX in either E/R$^+$ Ba/F3 or control cells, while in the presence of IL6/TNFα/IL1β levels of γH2AX significantly increased in both groups (γH2AX MFI fold increase + MSC+INFL.CK *vs* + MSC: E/R$^+$ = 2·28 ± 1·56, $P < 0{\cdot}05$; ctr = 4·36 ± 1·61, $P < 0{\cdot}01$).

Deregulation of activation-induced cytidine deaminase (AID) is a possible mechanism driving E/R$^+$ pre-leukemia to leukemia transition *in vivo* (Swaminathan *et al*, 2015). As shown in Fig 7B, pre-leukemic Ba/F3 basally expressed higher levels of AID mRNA compared to controls (AID mRNA fold increase: E/R$^+$ *vs* ctr = 4·9 ± 2·1, $P < 0{\cdot}05$). Very interestingly, AID expression further increased in both control and E/R$^+$ Ba/F3 once exposed to the inflamed niche secretome (AID mRNA fold increase + MSC+infl.ck *versus* basal: ctr = 14·7 ± 10·9, $P < 0{\cdot}05$; E/R$^+$=6·3 ± 1·6). However, further experiments are needed to functionally assess this observation.

Discussion

Dysregulated inflammatory and immune responses to common infections are the main candidate risk-factors for pre-leukemia to leukemia transition in BCP-ALL (Heath & Hasterlik, 1963; Francis *et al*, 2012; Cazzaniga *et al*, 2017). Here, we show that BM-MSC cooperate with IL6/TNFα/IL1β pro-inflammatory cytokines in favoring the persistence of E/R-expressing Ba/F3 as well as human CD34$^+$IL7R$^+$ progenitors, recently indicated as a putative E/R$^+$ leukemia initiating population during human development (Böiers *et al*, 2018).

IL6, TNFα and IL1β are pleiotropic cytokines precociously secreted by pathogen receptors (PRRs)-expressing cells in response to several types of infections (Swiergiel & Dunn, 1999). In addition to regulating normal HSPC under infective conditions (Riether *et al*, 2015), they contribute to the establishment and maintenance of the leukemic niche (Kagoya *et al*, 2014; Vilchis-Ordoñez *et al*, 2015; Carey *et al*, 2017). Notably, no advantaging effect was observed on pre-leukemic clone by treating the competitive E/R$^+$:ctr Ba/F3 mix with IL6/IL1β/TNFα in the absence of BM-MSC, indicating that the emergence of pre-leukemic cells against controls strictly depends on IL6/IL1β/TNFα-mediated mesenchymal inflammation. At the same time, treating the competitive mesenchymal niche with LPS, an infective stimulus prompting E/R leukemogenesis in mice (Swaminathan *et al*, 2015), did not increase the relative percentage of E/R$^+$ Ba/F3 against the normal counterpart. Discrepancy may be explained by supposing that LPS affects other niche component *in vivo* or indirectly acts on BM-MSC: for example, by stimulating antigen-presenting cells to secrete IL6/IL1β/TNFα (Swiergiel & Dunn, 1999).

By transwell experiments, we have evidence that soluble molecules are the main determinants of the pre-leukemia advantage within the inflamed niche. Regarding this, we previously demonstrated that TGFβ, a key immune modulator produced during inflammation (Yoshimuta *et al.*, 2010),

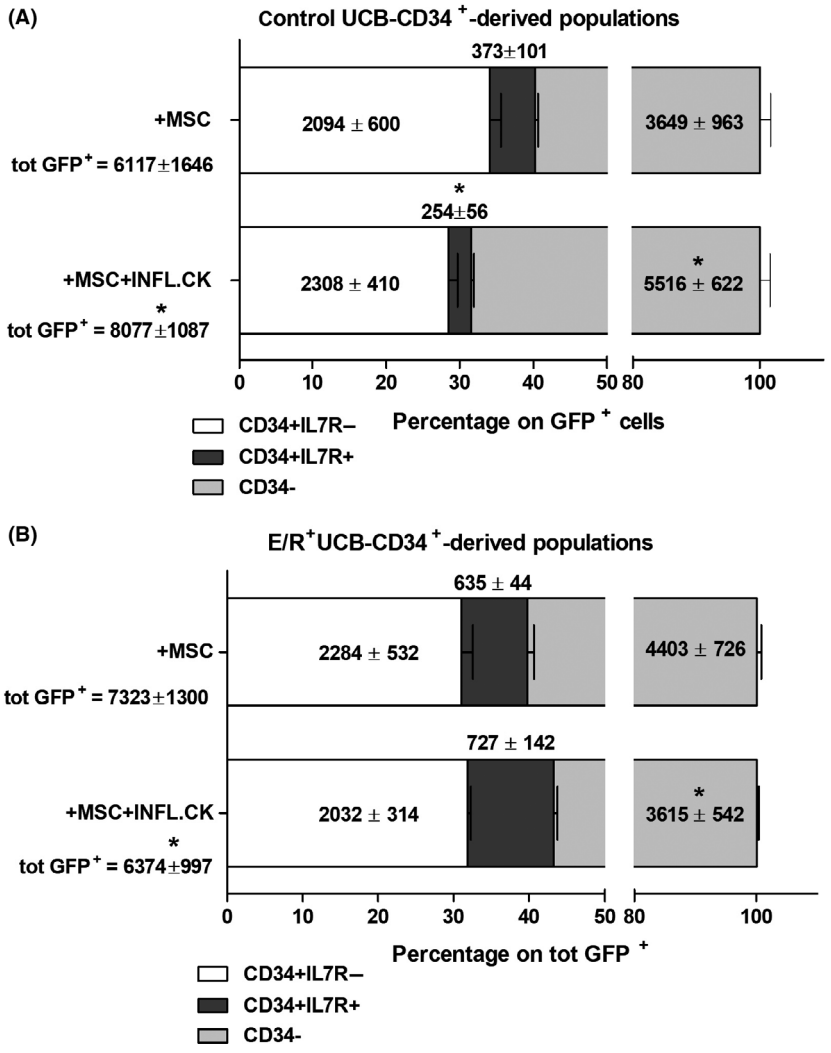

Fig 6. ETV6/RUNX1 safeguards the number of human $CD34^+IL7R^+$ in the presence of BM-MSC and inflammation. Transfected control and E/R-expressing human UCB-$CD34^+$ cells were separately grown in stem culture medium on BM-MSC in the absence (+MSC) or presence of IL6 (40 ng/mL), TNFα (100 ng/mL) and IL1β (50ng/mL) (+MSC + INFL.CK) for 72 h. At the end of the culture, cells were stained with anti-CD34 and anti-IL7Rα antibodies and counted by FACS. The cell number was normalized to a determined number of fluorescent reference beads (BD Trucount® tubes) added into tubes and to the percentage of GFP positivity in the two groups. Percentages of $CD34^-$, $CD34^-IL7R^+$ and $CD34^+IL7R^+$ fractions in control UCB-$CD34^+$-derived population (A) and in E/R^+ UCB-$CD34^+$-derived population (B) after 72 h of culture at the indicated conditions. Values indicate the number of cells relatively quantified by flow cytometry (mean ± SD of one infection experiment in which cells were cultivated on three different healthy donor-derived BM-MSC). Paired Student's *t*-test: * = same experimental group, inflamed *vs* non-inflamed condition; # = same experimental condition, control *vs* E/R^+ group; two-sided, $^{*,\#}P < 0{\cdot}05$; $^{\#\#}P < 0{\cdot}01$.

reduced proliferation in control but not E/R-expressing Ba/F3 (Ford *et al.*, 2009). However, IL6/IL1β/TNFα-stimulated BM-MSC do not increase TGFβ secretion compared to unstimulated cells. More recently, Böiers *et al.* (2018) showed that human E/R-expressing fetal pro-B cells can survive in myeloid culture conditions. Despite E/R^+ Ba/F3 transcriptionally activate inflammatory myeloid pathways and inflamed human BM-MSC release myeloid factors (data not shown), preliminary ongoing experiments seem to rule out their role in our observations.

CXCL1 was the most upregulated protein in the supernatants of inflamed compared to unstimulated BM-MSC; on the other hand, pre-leukemic Ba/F3 and patient-derived E/R^+ blasts overexpress its receptor CXCR2. Although CXCR2 does not directly favor the emergence of pre-leukemic cells within the inflamed mesenchymal niche, it is responsible for the preferential migration of E/R-expressing cells toward the sustaining niche, thus becoming a possible future therapeutic target (Ijichi *et al*, 2011; Martz, 2012; Schinke *et al*, 2015; Jaffer & Ma, 2016).

It is well established that additional mutations are required to complete malignant transformation of E/R^+ pre-leukemic cells (Greaves, 2018). Very interestingly, we demonstrate that exposure to the inflamed niche increased both the extent of DNA DSB and AID mRNA in E/R^+ Ba/F3. Although an effective role of AID in leukemia transition of B-cell precursors has yet to be proven, the increase of DNA damage observed in the apoptosis-resistant pre-leukemic clone could provide a means for their malignant transformation.

In conclusion, we propose a model where the concerted action of pro-inflammatory cytokines and BM-MSC creates a selective niche for E/R-expressing cells in terms of migration, proliferation and survival. In addition, the inflamed niche predisposes pre-leukemic cells to transformation by increasing DNA damage. Further characterization of the crucial pathways sustaining E/R^+ pre-leukemic cells within the inflamed niche could provide mechanistic insights into E/R-driven pathogenesis and, possibly, novel therapeutic interventions.

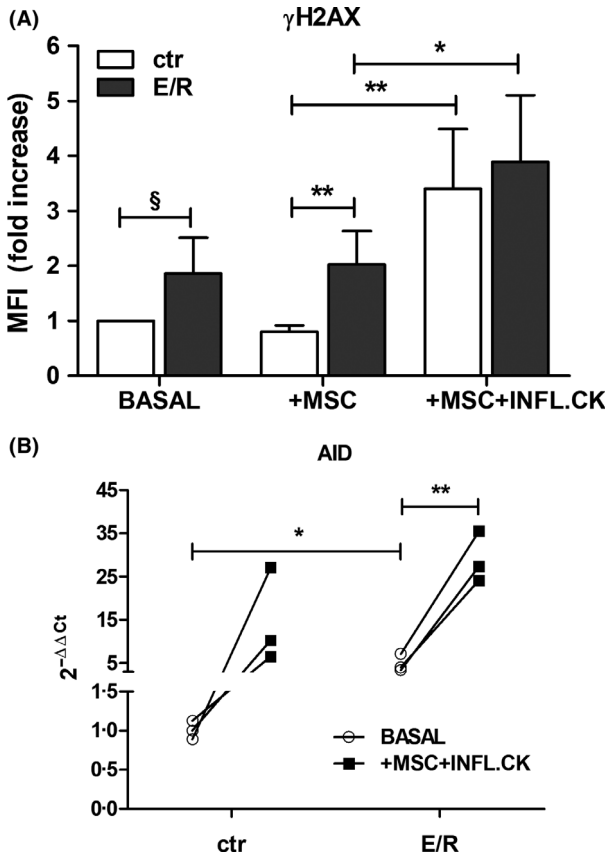

Fig 7. The inflamed mesenchymal niche increases DNA double-strand breaks and AID expression in both control and E/R$^+$ Ba/F3 cells. A) E/R$^+$ and control Ba/F3 cells were co-cultured (80%:20%) for 4 days in standard liquid culture (basal) or on murine BM-MSC monolayers in the presence or absence of IL6/TNFα/IL1β. Phosphorylated levels of H2AX (γH2AX) in mCD45$^+$, both V5-positive and V5-negative, cells were measured as MFI by FACS. The MFI of control Ba/F3 cells grown under basal condition was considered as reference for fold increase calculation. Values are expressed as mean ± SD of 6 independent experiments. One-sample *t*-test: $^{\S}P < 0{\cdot}05$. Paired Student's *t*-test: $^{*}P < 0{\cdot}05$; $^{**}P < 0{\cdot}01$. B) Control and E/R$^+$ Ba/F3 cells were separately grown in standard liquid culture (basal) or loaded into the upper chamber of 0·4 μm Transwell® inserts in the presence of MSC (lower chamber) and inflammatory cytokines (+MSC + INFL.CK). RT-qPCR analysis was performed to quantify AID expression, normalizing values on *Hprt* expression. Analysis was performed on 3 independent experiments. Paired Student's *t*-test: two-sided, $^{*}P < 0{\cdot}05$; $^{**}P < 0{\cdot}01$.

Acknowledgements

L.B. designed the study, performed experiments, collected and analyzed data and wrote the manuscript; E.D. contributed to the experimental design, provided murine BM-MSC and BM-MSC related protocols and revised the manuscript; C.B and P.M. provided scientific and logistical support for lentivirus production and human UCB-CD34+ cells infection; M.B. and D.A. performed experiments; A.F. provided the inducible Ba/F3 model and revised the manuscript; B.G. provided experimental support; S.B. and G.T. performed and analysed gene expression profile experiments; P.V. provided cord blood units; A.B. supervised the research; G.d'A. contributed to the experimental design; C.P. designed the study, performed experiments, collected and analysed data and revised the manuscript; G.C. supervised the research and revised the manuscript; C.P. and C.G. equally contributed to the work.

The authors thank Dr Caserta Carolina for experimental support. This study was supported by grants from: Fondazione Tettamanti, Fondazione Cariplo (2018-0339), Associazione Italiana Ricerca sul Cancro (AIRC, project number IG 2018 Id. 21999, to G.C., and IG 2014 Id.15494 to G.d'A.), and the Beat Leukemia Foundation (www.beat-leukemia.org). L.B. was supported by scholarships from Bianchi Industrial and Società Italiana Ematologia Sperimentale (SIES). The laboratory work by P.M. was funded by the European Research Council (CoG-2014-646903 and PoC-2018-811220), the Agencia Estatal de Investigación/European Regional Development Fund (SAF2016-80481-R and SAF2016-75442-R) and the Catalunya Government (SGR330 and PERIS 2017) to P.M; the laboratory work by and C.B. was funded by the Asociación Española Contra el Cáncer, Beca FERO and the ISCIII/FEDER (PI17/01028). P.M also acknowledges the institutional support from the Obra Social La Caixa-Fundaciò Josep Carreras.

Conflict of Interest

The authors declare no competing financial interests.

Authors' disclosures of potential conflicts of interest

There are no conflicts of interest to disclose.

Supporting Information

Additional supporting information may be found online in the Supporting Information section at the end of the article.

Figure S1. Schematic representation of the competitive niche assay.

Figure S2. The competitive niche assay in the presence of several stimuli.

Figure S3. LPS stimulation does not provide advantage to E/R$^+$ Ba/F3 in the competitive mesenchymal niche.

Figure S4. Soluble factors, other than TGFβ, mediate the pre-leukemia selective advantage within the inflamed mesenchymal niche.

Figure S5. A) Gene expression profiling by Gene Chip Mouse 2.0 Arrays of control and E/R$^+$ Ba/F3. Only those E/R induction experiments showing >90% viability and >90% FITC positivity were chosen for analysis ($n = 3$). B) E/R$^+$ Ba/F3 upregulated pathways involved in the immune and inflammatory response, included myeloid cell activation pathways. Gene ontology (GO) analysis was performed by

Metascape. Differentially expressed genes were identified by significance analysis of microarray (SAM) algorithm coded in the samr R package and by estimating the percentage of false positive predictions (i.e. false discovery rate, FDR) with 100 permutations; *q-value <0.01*. In the dendogram, the 20 best *p*-values are indicated. C) Signaling associated to IL-8, a CXCR2-ligand, was one of the top canonical pathways upregulated in pre-leukemic cells. Ingenuity Pathway Analysis was performed on filtered GEP data (E/R$^+$ *versus* control Ba/F3: FC < 0.75 and FC > 1.5). As evidenced, the IL-8 signaling was activated in pre-leukemic Ba/F3 compared to controls.

Figure S6. E/R$^+$ BCP-ALL patients overexpress *CXCR2* mRNA.

Figure S7. Inhibition of CXCR2 did not abolish the relative increase of pre-leukemic cells percentage within the inflamed niche.

Figure S8. CXCL1 does not provide a selective advantage to E/R$^+$ Ba/F3 in competitive liquid culture.

Figure S9. A) Representative plots for relative quantitative analysis of the CD34$^-$, CD34$^+$IL7R$^-$, CD34$^+$IL7R$^+$ and CD34^{high}IL7R$^+$ fractions within control and pre-leukemic GFP$^+$ populations. Control and E/R-transduced UCB-CD34$^+$ cells were separately grown in stem culture medium on BM-MSC, in absence (+MSC) or presence of IL6/TNFα/IL1β (+MSC+INFL.CK) for 72 h. At the end of the culture, cells were stained with APC-conjugated anti-hCD34 and PE-Cy7-conjugated anti-hIL7R antibodies and analyzed by quantitative flow cytometry. Plots show a representative phenotypic analysis of both cell groups after the cultivation on unstimulated BM-MSC. P4 = GFP$^+$; P5 = CD34$^+$IL7R$^+$; P6 = CD34$^+$IL7R$^-$; P7 = CD34$^-$; P8 = CD34^{high}IL7R$^+$. B) Human E/R$^+$ CD34^{high}IL7R$^+$ progenitors are preserved under mesenchymal inflammation. Control and E/R-transduced UCB-CD34$^+$ cells were separately grown in stem culture medium on BM-MSC, in absence (+MSC) or presence of IL6/TNFα/IL1β (+MSC+INFL.CK) for 72 h. At the end of the culture, cells were stained with the anti-hCD34 and anti-hIL7Rα antibodies and number of cells quantified by FACS. The cell number was normalized on a determined number of fluorescent reference beads (BD Trucount® tubes) and percentage of GFP positivity in the two groups. The graph shows results of one infection experiment in which cells were cultivated on three different healthy donor-derived BM-MSC monolayers. For every BM-MSC healthy donor, FC between the number of CD34^{high}IL7R$^+$ in the inflamed and unstimulated BM-MSC niche was calculated and the mean±SD indicated in the graph. One-sample *t*-test: $^{\S}P < 0.05$.

Table S1. BM-MSC from three different healthy donors were cultivated in 2% FBS-supplemented medium for 24 h in the presence or absence of IL1β, IL6 and TNFα. Collected supernatants were analyzed by Human Cytokines Array C1000 and Student's *t*-test was applied to compare inflamed *vs* unstimulated values. For each donor, the fold change (FC) between the two conditions was calculated.

Table S2. Gene expression profile by Gene Chip Mouse 2.0 Arrays of control and E/R+ Ba/F3 cells. E/R induction experiments showing >90% viability and FITC positivity were chosen ($n = 3$). Differentially expressed genes were identified by using Significance Analysis of Microarray algorithm (SAM) coded in the samr R package and estimating the percentage of false positive predictions (i.e., False Discovery Rate, FDR) with 100 permutations.

Table S3. General characteristics of patients whose cDNA were analyzed for *CXCR1/2* expression. Sixty-six BCP-ALL patients (32 E/R-positive patients and 34 patients negative for all common translocations), enrolled in the AIEOP-BFM ALL 2009 protocol and treated in AIEOP Centers, were included in the study. BCP-ALL diagnosis was performed according to standard cytomorphology, cytochemistry and immunophenotypic criteria. RNA were isolated from mononuclear cells and cDNA was synthesized according to standard methods.

Data S1. Supplementary materials.

References

Asada, N. (2018) Regulation of malignant Hematopoiesis by bone marrow microenvironment. *Frontiers in Oncology*, **8**, 119.

Bernardo, M.E. & Fibbe, W.E. (2013) Mesenchymal stromal cells: Sensors and switchers of inflammation. *Cell Stem Cell*, **13**, 392–402.

Böiers, C., Richardson, S.E., Laycock, E., Zriwil, A., Turati, V.A., Brown, J., Wray, J.P., Wang, D., James, C., Herrero, J., Sitnicka, E., Karlsson, S., Smith, A.J.H., Jacobsen, S.E.W. & Enver, T. (2018) A human IPS model implicates embryonic B-myeloid fate restriction as developmental susceptibility to B acute lymphoblastic leukemia-associated ETV6-RUNX1. *Developmental Cell*, **44**, 362–377.

Cappuzzello, C., Doni, A., Dander, E., Pasqualini, F., Nebuloni, M., Bottazzi, B., Mantovani, A., Biondi, A., Garlanda, C. & D'Amico, G. (2016) Mesenchymal stromal cell-derived PTX3 promotes wound healing via fibrin remodeling. *The Journal of Investigative Dermatology*, **136**, 293–300.

Carey, A., Edwards, D.K., Eide, C.A., Newell, L., Traer, E., Medeiros, B.C., Pollyea, D.A., Deininger, M.W., Collins, R.H., Tyner, J.W., Druker, B.J., Bagby, G.C., McWeeney, S.K. & Agarwal, A. (2017) Identification of interleukin-1 by functional screening as a key mediator of cellular expansion and disease progression in acute myeloid leukemia. *Cell Reports*, **18**, 3204–3218.

Cazzaniga, G., Bisanti, L., Randi, G., Deandrea, S., Bungaro, S., Pregliasco, F., Perotti, D., Spreafico, F., Masera, G., Valsecchi, M.G., Biondi, A. & Greaves, M. (2017) Possible role of pandemic AH1N1 swine flu virus in a childhood leukemia cluster. *Leukemia*, **31**, 1819–1821.

De Rooij, B., Polak, R., Van Den Berk, L.C.J., Stalpers, F., Pieters, R. & Den Boer, M.L. (2017) Acute lymphoblastic leukemia cells create a leukemic niche without affecting the CXCR4/CXCL12 axis. *Haematologica*, **102**, e389–e393.

Diakos, C., Krapf, G., Gerner, C., Inthal, A., Lemberger, C., Ban, J., Dohnal, A.M. & Panzer-Gruemayer, E.R. (2007) RNAi-mediated silencing of TEL/AML1 reveals a heat-shock protein- and survivin-dependent mechanism for survival. *Blood*, **109**, 2607–2610.

Ford, A.M., Bennett, C.A., Price, C.M., Bruin, M.C., Van Wering, E.R. & Greaves, M. (1998) Fetal origins of the TEL-AML1 fusion gene in identical twins with leukemia. *Proceedings of the National Academy of Sciences of the United States of America*, **95**, 4584–4588.

Ford, A.M., Fasching, K., Panzer-Grümayer, E.R., Koenig, M., Haas, O.A. & Greaves, M.F. (2001)

Origins of 'late' relapse in childhood acute lymphoblastic leukemia with TEL-AML1 fusion genes. *Blood*, **98**, 558–564.

Ford, A.M., Palmi, C., Bueno, C., Hong, D., Cardus, P., Knight, D., Cazzaniga, G., Enver, T. & Greaves, M. (2009) The TEL-AML1 leukemai fusion gene dysregulates the TGF-beta pathway in early B lineage progenitor cells. *Journal of Clinical Investigation*, **119**, 826–836.

Francis, S.S., Selvin, S., Yang, W., Buffler, P.A. & Wiemels, J.L. (2012) Unusual space-time patterning of the Fallon, Nevada leukemia cluster: Evidence of an infectious etiology. *Chemico-Biological Interactions*, **196**, 102–109.

Golub, T.R., Barker, G.F., Bohlander, S.K., Hiebert, S.W., Ward, D.C., Bray-Ward, P., Morgan, E., Raimondi, S.C., Rowley, J.D. & Gilliland, D.G. (1995) Fusion of the TEL gene on 12p13 to the AML1 gene on 21q22 in acute lymphoblastic leukemia. *Proceedings of the National Academy of Sciences*, **92**, 4917–4921.

Greaves, M. (2018) A causal mechanism for childhood acute lymphoblastic leukaemia. *Nature Reviews Cancer*, **18**, 471–484.

Heath, C.W. & Hasterlik, R.J. (1963) Leukemia among children in a suburban community. *The American Journal of Medicine*, **34**, 796–812.

Hong, D., Gupta, R., Ancliff, P., Atzberger, A., Brown, J., Soneji, S., Green, J., Colman, S., Piacibello, W., Buckle, V., Tsuzuki, S., Greaves, M. & Enver, T. (2008) Initiating and cancer-propagating cells in TEL-AML1-associated childhood leukemia. *Science*, **319**, 336–339.

Ijichi, H., Chytil, A., Gorska, A.E., Aakre, M.E., Bierie, B., Tada, M., Mohri, D., Miyabayashi, K., Asaoka, Y., Maeda, S., Ikenoue, T., Tateishi, K., Wright, C.V.E., Koike, K., Omata, M. & Moses, H.L. (2011) Inhibiting Cxcr2 disrupts tumor-stromal interactions and improves survival in a mouse model of pancreatic ductal adenocarcinoma. *Journal of Clinical Investigation*, **121**, 4106–4117.

Inaba, H., Greaves, M. & Mullighan, C.G. (2013) Acute lymphoblastic leukaemia. *The Lancet*, **381**, 1943–1955.

Jaffer, T. & Ma, D. (2016) The emerging role of chemokine receptor CXCR2 in cancer progression. *Translational Cancer Research*, **5**, S616–S628.

Kagoya, Y., Yoshimi, A., Kataoka, K., Nakagawa, M., Kumano, K., Arai, S., Kobayashi, H., Saito, T., Iwakura, Y. & Kurokawa, M. (2014) Positive feedback between NF-κB and TNF-α promotes leukemia-initiating cell capacity. *Journal of Clinical Investigation*, **124**, 528–542.

Kantner, H.-P., Warsch, W., Delogu, A., Bauer, E., Esterbauer, H., Casanova, E., Sexl, V. & Stoiber, D. (2013) ETV6/RUNX1 induces reactive oxygen species and drives the accumulation of DNA damage in B Cells. *Neoplasia*, **15**, 1292–1300.

Konrad, M., Metzler, M., Panzer, S., O¨ streicher, I., Peham, M., Repp, R., Haas, O.A., Gadner, H., Panzer-Gru¨mayer, E.R.. & TEL/AML1-positive (2003) Late relapses evolve from slow-responding subclones acute lymphoblastic leukemia : for the persistence evidence of a preleukemic clone. 101, 3635–3640.

Kuster, L., Grausenburger, R., Fuka, G., Kaindl, U., Krapf, G., Inthal, A., Mann, G., Kauer, M., Rainer, J., Kofler, R., Hall, A., Metzler, M., Meyer, D.H., Meyer, C., Harbott, J., Marschalek, R., Strehl, S., Haas, O.A., Panzer-gru, R. & Runx, E.T.V. (2018) ETV6_RUNX1-positive relapses evolve from an ancestral clone and frequently acquire deletions of genes implicated in glucocorticoid signalling. *Blood*. **117**, 2658–2668.

Levasseur, M., Maung, Z.T., Jackson, G.H., Kernahan, J., Proctor, S.J. & Middleton, P.G. (1994) Relapse of acute lymphoblastic leukaemia 14 years after presentation: Use of molecular techniques to confirm true re-emergence. *British Journal of Haematology*, **87**, 437–438.

Lilly, A.J., Johnson, W.E. & Bunce, C.M. (2011) The haematopoietic stem cell niche: New insights into the mechanisms regulating haematopoietic stem cell behaviour. *Stem Cells International*, **2011**, 1–10.

Linka, Y., Ginzel, S., Krüger, M., Novosel, A., Gombert, M., Kremmer, E., Harbott, J., Thiele, R., Borkhardt, A. & Landgraf, P. (2013) The impact of TEL-AML1 (ETV6-RUNX1) expression in precursor B cells and implications for leukaemia using three different genome-wide screening methods. *Blood Cancer Journal*, **3**, e151.

Lo, V., Ramı, M., Moreno, I.C. & Garcı, J. (2014) Mesenchymal Stromal Cells Derived from the Bone Marrow of Acute Lymphoblastic Leukemia Patients Show Altered BMP4 Production : Correlations with the Course of Disease. **9,** 1–11.

Martz, L. (2012) CXCR2 antagonists in breast cancer. *Science-Business eXchange*, **5**, 1–2.

Méndez-Ferrer, S., Michurina, T.V., Ferraro, F., Mazloom, A.R., MacArthur, B.D., Lira, S.A., Scadden, D.T., Ma'ayan, A., Enikolopov, G.N. & Frenette, P.S. (2010) Mesenchymal and haematopoietic stem cells form a unique bone marrow niche. *Nature*, **466**, 829–834.

Mullighan, C.G. (2013) Genomic characterization of childhood acute lymphoblastic leukemia. *Seminars in Hematology*, **50**, 314–324.

Naderi, E.H., Skah, S., Ugland, H., Myklebost, O., Sandnes, D.L., Torgersen, M.L., Josefsen, D., Ruud, E., Naderi, S. & Blomhoff, H.K. (2015) Bone marrow stroma-derived PGE2 protects BCP-ALL cells from DNA damage-induced p53 accumulation and cell death. *Molecular Cancer*, **14**, 1–14.

Palmi, C., Fazio, G., Savino, A.M., Procter, J., Howell, L., Cazzaniga, V., Vieri, M., Longinotti, G., Brunati, I., Andrè, V., Della Mina, P., Villa, A., Greaves, M., Biondi, A., D'Amico, G., Ford, A. & Cazzaniga, G. (2014) Cytoskeletal regulatory gene expression and migratory properties of B-cell progenitors are affected by the ETV6-RUNX1 rearrangement. *Molecular cancer research*, **12**, 1796–806.

Polak, R., De Rooi, B. & Pieters, R. (2015) B-cell precursor acute lymphoblastic leukemia cells use tunneling nanotubes to orchestrate their microenvironment. *Blood*, **126**, 2404–2414.

Portale, F., Cricrì, G., Bresolin, S., Lupi, M., Gaspari, S., Silvestri, D., Russo, B., Marino, N., Ubezio, P., Pagni, F., Vergani, P., Kronnie, G.T., Valsecchi, M.G., Locatelli, F., Rizzari, C., Biondi, A., Dander, E. & D'Amico, G. (2019) ActivinA: a new leukemia-promoting factor conferring migratory advantage to B-cell precursor-acute lymphoblastic leukemic cells. *Haematologica*, **104**, 533–545.

Raaijmakers, M.H.G.P., Mukherjee, S., Guo, S., Zhang, S., Kobayashi, T., Schoonmaker, J.A., Ebert, B.L., Al-Shahrour, F., Hasserjian, R.P., Scadden, E.O., Aung, Z., Matza, M., Merkenschlager, M., Lin, C., Rommens, J.M. & Scadden, D.T. (2010) Bone progenitor dysfunction induces myelodysplasia and secondary leukaemia. *Nature*, **464**, 852–857.

Richardson, R.M., Marjoram, R.J., Barak, L.S. & Snyderman, R. (2003) Role of the cytoplasmic tails of CXCR1 and CXCR2 in mediating leukocyte migration, activation, and regulation. *The Journal of Immunology*, **170**, 2904–2911.

Riether, C., Schürch, C.M. & Ochsenbein, A.F. (2015) Regulation of hematopoietic and leukemic stem cells by the immune system. *Cell Death and Differentiation*, **22**, 187–198.

Rodríguez-Hernández, G., Hauer, J., Martín-Lorenzo, A., Schäfer, D., Bartenhagen, C., García-Ramírez, I., Auer, F., Gonzalez-Herrero, I., Ruiz-Roca, L., Gombert, M., Okpanyi, V., Fischer, U., Chen, C., Dugas, M., Bhatia, S., Linka, R.M., Garcia-Suquia, M., Rascón-Trincado, M.V., Garcia-Sanchez, A., Blanco, O., García-Cenador, M.B., García-Criado, F.J., Cobaleda, C., Alonso-López, D., De Las Rivas, J., Müschen, M., Vicente-Dueñas, C., Sánchez-García, I. & Borkhardt, A. (2017) Infection exposure promotes ETV6-RUNX1 precursor B-cell leukemia via impaired H3K4 demethylases. *Cancer Research*, **77**, 4365–4377.

Romana, S.P., Mauchauffe, M., Le Coniat, M., Le Paslier, D., Berger, R. & Bernard, O.A. (1995) The t(12;21) of acute lymphoblastic leukemia results in a tel-AML1 gene fusion. *Blood*, **85**, 3662–3670.

Rosu-Myles, M., Khandaker, M., Wu, D.M., Keeney, M., Foley, S.R., Howson-Jan, K., Yee, I.C., Fellows, F., Kelvin, D. & Bhatia, M. (2000) Characterization of chemokine receptors expressed in primitive blood cells during human hematopoietic ontogeny. *Stem Cells*, **18**, 374–381.

Schäfer, D., Olsen, M., Lähnemann, D., Stanulla, M., Slany, R., Schmiegelow, K., Borkhardt, A. & Fischer, U. (2018) Five percent of healthy newborns have an ETV6-RUNX1 fusion as revealed by DNA-based GIPFEL screening. *Blood*, **15**, 821–826.

Schindler, J.W., Van Buren, D., Foudi, A., Krejci, O., Qin, J., Orkin, S.H. & Hock, H. (2009) TEL-AML1 corrupts hematopoietic stem cells to persist in the bone marrow and initiate leukemia. *Cell Stem Cell*, **5**, 43–53.

Schinke, C., Giricz, O., Li, W., Shastri, A., Gordon, S., Barreyro, L., Bhagat, T., Bhattacharyya, S., Ramachandra, N., Bartenstein, M., Pellagatti, A., Boultwood, J., Wickrema, A., Yu, Y., Will, B., Wei, S., Steidl, U. & Verma, A. (2015) IL8-CXCR2 pathway inhibition as a therapeutic strategy against MDS and AML stem cells. *Blood*, **125**, 3144–3152.

Scutera, S., Salvi, V., Lorenzi, L., Piersigilli, G., Lonardi, S., Alotto, D., Casarin, S., Castagnoli, C., Dander, E., D'Amico, G., Sozzani, S. & Musso, T. (2018) Adaptive regulation of osteopontin production by dendritic cells through the bidirectional interaction with mesenchymal stromal cells. *Frontiers in Immunology*, **9**, 1207.

Sinclair, A., Park, L., Shah, M., Drotar, M., Calaminus, S., Hopcroft, L.E.M., Kinstrie, R., Guitart, A.V., Dunn, K., Abraham, S.A., Sansom, O., Michie, A.M., Machesky, L., Kranc, K.R., Graham, G.J., Pellicano, F. & Holyoake, T.L. (2016) CXCR2 and CXCL4 regulate survival and self-renewal of hematopoietic stem/progenitor cells. *Blood*, **128**, 371–383.

Stillie, R., Farooq, S.M., Gordon, J.R. & Stadnyk, A.W. (2009) The functional significance behind expressing two IL-8 receptor types on PMN. *Journal of Leukocyte Biology*, **86**, 529–543.

Swaminathan, S., Klemm, L., Park, E., Papaemmanuil, E., Ford, A., Kweon, S.M., Trageser, D., Hasselfeld, B., Henke, N., Mooster, J., Geng, H., Schwarz, K., Kogan, S.C., Casellas, R., Schatz, D.G., Lieber, M.R., Greaves, M.F. & Müschen, M. (2015) Mechanisms of clonal evolution in childhood acute lymphoblastic leukemia. *Nature Immunology*, **16**, 766–774.

Swiergiel, A.H. & Dunn, A.J. (1999) The roles of IL-1, IL-6, and TNFα in the feeding responses to endotoxin and influenza virus infection in mice. *Brain, Behavior, and Immunity*, **13**, 252–265.

Tsuzuki, S., Seto, M., Greaves, M. & Enver, T. (2004) Modeling first-hit functions of the t (12;21) TEL-AML1 translocation in mice. *Proceedings of the National Academy of Sciences*, **101**, 8443–8448.

Vilchis-Ordoñez, A., Contreras-Quiroz, A., Vadillo, E., Dorantes-Acosta, E., Reyes-López, A., Quintela-Nuñez Del Prado, H.M., Venegas-Vázquez, J., Mayani, H., Ortiz-Navarrete, V., López-Martínez, B. & Pelayo, R. (2015) Bone marrow cells in acute lymphoblastic leukemia create a proinflammatory microenvironment influencing normal hematopoietic differentiation fates. *BioMed Research International*, **2015**, 1–14.

Wiemels, J.L., Cazzaniga, G., Daniotti, M., Eden, O.B., Addison, G.M., Masera, G., Saha, V., Biondi, A. & Greaves, M.F. (1999) Prenatal origin of acute lymphoblastic leukaemia in children. *Lancet*, **354**, 1499–1503.

Yoshimura, A., Wakabayashi, Y. & Mori, T. (2010) Cellular and molecular basis for the regulation of inflammation by TGF-β. *Journal of Biochemistry*, **147**, 781–792.

Zambetti, N.A., Ping, Z., Chen, S., Kenswil, K.J.G., Mylona, M.A., Sanders, M.A., Hoogenboezem, R.M., Bindels, E.M.J., Adisty, M.N., Van Strien, P.M.H., van der Leije, C.S., Westers, T.M., Cremers, E.M.P., Milanese, C., Mastroberardino, P.G., van Leeuwen, J.P.T.M., van der Eerden, B.C.J., Touw, I.P., Kuijpers, T.W., Kanaar, R., van de Loosdrecht, A.A., Vogl, T. & Raaijmakers, Marc HGP (2016) Mesenchymal inflammation drives genotoxic stress in hematopoietic stem cells and predicts disease evolution in human pre-leukemia. *Cell Stem Cell*, **19**, 613–627.